



Re-targeting of a plant defense protease by a cyst nematode effector

Gennady V. Pogorelko¹, Parijat S. Juvale¹, William B. Rutter², Marion Hütten³, Thomas R. Maier¹, Tarek Hewezi⁴, Judith Paulus⁵, Renier AL van der Hoorn⁵, Florian MW Grundler³, Shahid Siddique^{3,†} , Vincenzo Lionetti⁶, Olga A. Zabolina⁷ and Thomas J. Baum^{1,*} 

¹Department of Plant Pathology and Microbiology, Iowa State University, Ames, IA 50011, USA,

²USDA-ARS, US Vegetable Laboratory, 2700 Savannah Highway, Charleston, SC 29414, USA,

³Rheinische Friedrich-Wilhelms-University Bonn, INRES – Molecular Phytomedicine, Bonn, Germany,

⁴Department of Plant Sciences, University of Tennessee, Knoxville, TN 37996, USA,

⁵Plant Chemetics Laboratory, Department of Plant Sciences, University of Oxford, Oxford, UK,

⁶Dipartimento di Biologia e Biotechnologie, Charles Darwin, Sapienza Università di Roma, 00185, Rome, Italy, and

⁷Roy J. Carver Department of Biochemistry, Biophysics, and Molecular Biology, Iowa State University, Ames, IA 50011, USA

Received 23 March 2018; revised 8 February 2019; accepted 15 February 2019.

*For correspondence (e-mail tbaum@iastate.edu).

†Current address: Department of Entomology and Nematology, University of California, Davis, CA 95616, USA.

SUMMARY

Plants mount defense responses during pathogen attacks, and robust host defense suppression by pathogen effector proteins is essential for infection success. 4E02 is an effector of the sugar beet cyst nematode *Heterodera schachtii*. *Arabidopsis thaliana* lines expressing the effector-coding sequence showed altered expression levels of defense response genes, as well as higher susceptibility to both the biotroph *H. schachtii* and the necrotroph *Botrytis cinerea*, indicating a potential suppression of defenses by 4E02. Yeast two-hybrid analyses showed that 4E02 targets *A. thaliana* vacuolar papain-like cysteine protease (PLCP) 'Responsive to Dehydration 21A' (RD21A), which has been shown to function in the plant defense response. Activity-based protein profiling analyses documented that the *in planta* presence of 4E02 does not impede enzymatic activity of RD21A. Instead, 4E02 mediates a re-localization of this protease from the vacuole to the nucleus and cytoplasm, which is likely to prevent the protease from performing its defense function and at the same time, brings it in contact with novel substrates. Yeast two-hybrid analyses showed that RD21A interacts with multiple host proteins including enzymes involved in defense responses as well as carbohydrate metabolism. In support of a role in carbohydrate metabolism of RD21A after its effector-mediated re-localization, we observed cell wall compositional changes in 4E02 expressing *A. thaliana* lines. Collectively, our study shows that 4E02 removes RD21A from its defense-inducing pathway and repurposes this enzyme by targeting the active protease to different cell compartments.

Keywords: effector, nematode, plant–pathogen interaction, protease, re-localization, defense.

INTRODUCTION

Nematodes are animals occupying a broad range of ecological niches including plant parasitism (Cobb, 1914). The most important group of plant-parasitic nematodes contains the cyst nematodes (*Heterodera* and *Globodera* species), which cause billions of dollars in yield loss by infecting economically important crops (Koenning and Wrather, 2010). Cyst nematodes invade plant roots and migrate intracellularly toward the vascular tissue where they induce the formation of specialized feeding sites (syncytia) consisting of fused, modified root cells.

Nematode-directed re-differentiation of root cells to form syncytia as well as effective suppression of plant defense mechanisms constitute the basis of successful cyst nematode parasitism (Mitchum *et al.*, 2013). The comprehensive cellular re-programming at the infection site, as well as the robust and long-term host defense suppression necessary for successful parasitism, is thought to be achieved by a suite of effectors secreted by nematodes. Dozens of such effector proteins produced in the esophageal gland cells of nematodes have been identified (Gao

et al., 2001, 2003; Vanholme et al., 2006; Noon et al., 2015). Published reports confirm that these effector proteins, delivered to the infection site through a hollow stylet by the invading nematodes, target distinct cellular compartments such as nuclei, cytoplasm, and the apoplast, where they execute virulence functions by interacting with host factors (Hewezi and Baum, 2013; Mitchum et al., 2013; Hewezi, 2015; Habash et al., 2017a,b; Juvale and Baum, 2018). Evidence of host proteins being targeted by cyst nematode effectors to perform virulence functions has been well documented. Although discovery of effector-interacting host proteins has shed light on the intricate molecular interactions between the host and nematodes, we are still at an early stage of understanding this complex phenomenon, as many of the cyst nematode effectors remain uncharacterized and without predicted functions.

4E02 is one such effector that was first identified as a transcript predicted to encode an approximately 7.5 kDa protein containing an N-terminal signal peptide for secretion and that is specifically expressed within the subventral esophageal gland cells of the soybean cyst nematode *Heterodera glycines* (Gao et al., 2003). The esophageal gland cells are a primary source of secreted effector proteins (Hussey, 1989). Similar to many other putative effector proteins identified from *H. glycines*, 4E02 has no homologues within the NCBI database and contains no known protein domains with the exception of a SV40-type nuclear localization signal (NLS). The functionality of this NLS was confirmed experimentally by localizing 4E02 to the nuclei of onion epidermal cells and *A. thaliana* protoplasts (Elling et al., 2007).

In this current study, we build on the prior characterizations of 4E02 and present an in-depth functional study using

the *A. thaliana*–sugar beet cyst nematode (*H. schachtii*) pathosystem. Our results revealed that the 4E02 effector from *H. schachtii* (Hs4E02) achieves a virulence function by targeting and re-localizing the critical host protease ‘Responsive to Dehydration 21A’ (RD21A) in its active form that is associated with changes in the *A. thaliana* host immune response as well as cell wall compositional changes.

RESULTS

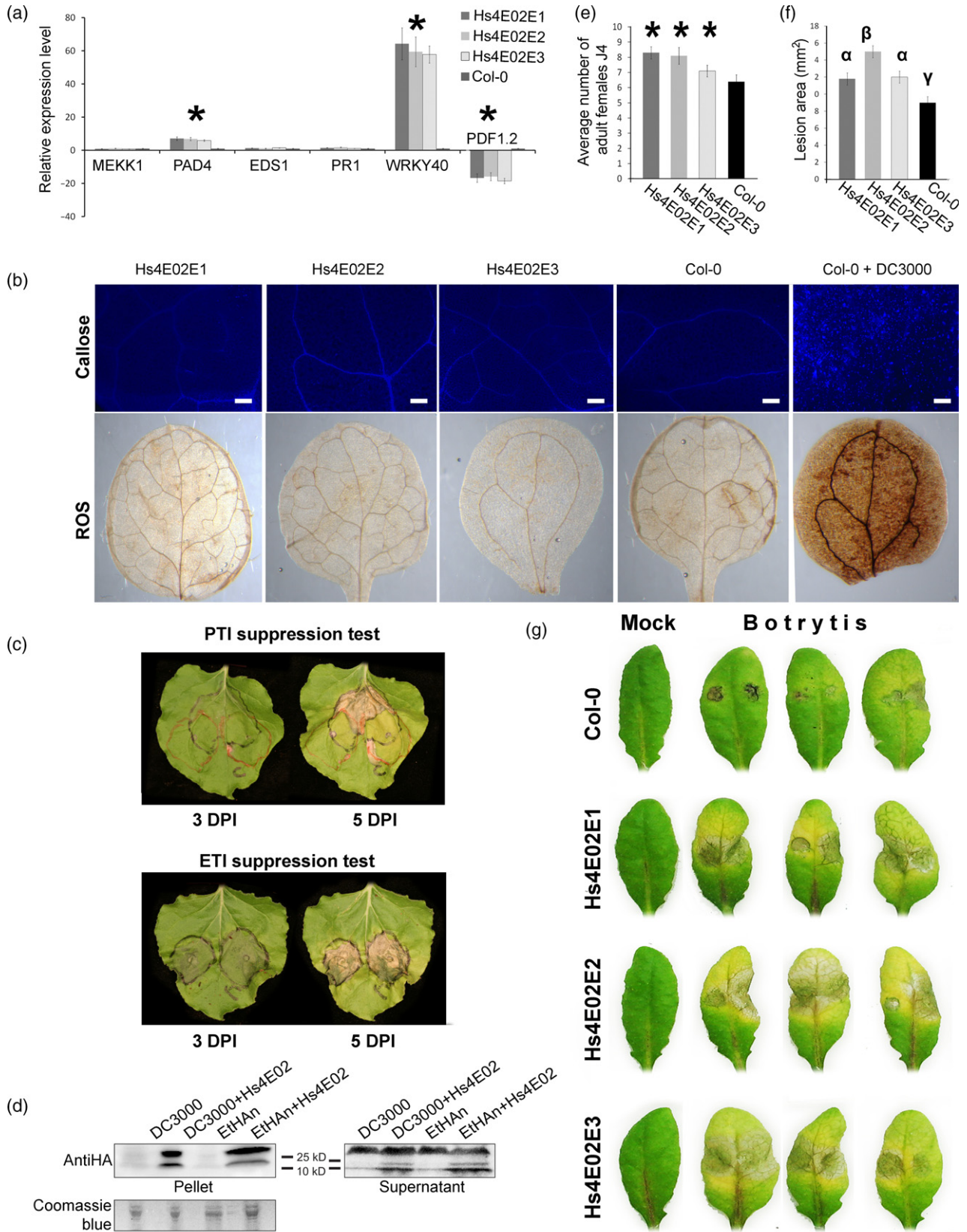
The effector Hs4E02 alters certain host defense responses and aids both biotrophic and necrotrophic pathogens

Cyst nematodes are obligatory, sedentary biotrophs that need to evade the plant immune response for an extended duration to complete their life cycle. As the Hs4E02 effector gene is expressed in esophageal glands during all stages of infection (Patel et al., 2008), we hypothesized that this effector has a role in the long-term modulation of plant defenses. This hypothesis is supported by a recently published report showing that cyst nematode effector GLAND18, whose gene is also constitutively expressed in the esophageal glands throughout all life stages of the cyst nematode, strongly suppresses plant innate immune responses (Noon et al., 2016).

To characterize Hs4E02 virulence functions, we generated stable transgenic *A. thaliana* lines (Hs4E02E) constitutively expressing the effector-coding sequence lacking the secretory signal peptide. The level of Hs4E02 mRNA expression was confirmed in three independent homozygous *A. thaliana* lines (Hs4E02E lines 1 to 3) using the quantitative reverse-transcription polymerase chain reaction (qRT-PCR) (Figure S1). These three lines were used in all subsequent experiments.

Figure 1. Constitutive expression of the Hs4E02 coding sequence in *Arabidopsis thaliana* alters host defense responses and cyst nematode susceptibility.

- (a) Expression analysis of the selected pathogenesis-related genes in Hs4E02E transgenic lines by real-time RT-PCR. Gene expression levels in transgenic plants normalized to the expression levels detected in non-transformed Col-0 plants. *Actin2* gene was used as an internal reference. Data are the average of three independent biological samples. Expression levels significantly different ($P < 0.05$) from controls as determined by paired *t*-test are denoted by asterisks.
- (b) Callose deposition (upper panel) and ROS accumulation (lower panel) in leaves of Hs4E02E lines. To detect callose deposition, detached leaves from uninfected transgenic and non-transformed Col-0 plants were stained with aniline blue and photographed under ultraviolet (UV) light. To detect ROS accumulation, detached leaves from uninfected transgenic and non-transformed Col-0 plants were stained with 3,3'-diaminobenzidine and photographed under visible light. The experiment was repeated multiple times and similar results were observed for each transgenic line. As a positive control for both callose and ROS tests, detached leaves of non-transformed Col-0 were infected with *Pseudomonas syringae* DC3000 and stained (last image in each panel). Bars = 200 μ m.
- (c) Basal immunity suppression experiments. For PTI suppression tests, wild-type EtHan (right side of the leaf) and EtHan + Hs4E02 (left side of the leaf) (both OD₆₀₀ = 0.2) were infiltrated into *Nicotiana benthamiana* leaves (black tracing) on opposite sides of the midrib, and after 6 h, challenge infiltrations were performed with wild-type *Pst* DC3000 (OD₆₀₀ = 0.02) (red tracing). Absence of HR caused by *Pst* DC3000 after 2 dpi within the overlapping areas for EtHan + Hs4E02, indicating unaffected basal immunity. For ETI suppression tests, wild-type *Pst* DC3000 (right side of the leaf) and *Pst* DC3000 + Hs4E02 (left side of the leaf) (both OD₆₀₀ = 0.02) were infiltrated into *N. benthamiana* leaves on opposite sides of the midrib, and images were taken at 3 dpi. Absence of difference in HR development indicates Hs4E02 does not alter ETI response.
- (d) Western blot showing specific expression of Hs4E02 in the pellet and supernatant for both *P. syringae* DC3000 and *Pseudomonas fluorescens* EtHan. Bacteria were cultured in HRP-inducing (type III secretion system) minimal medium. Anti (α)-HA antibody was used for the western blot and a strong band corresponding to Hs4E02 was present in all pellet samples. Coomassie blue stained gel was used as loading control. No Coomassie blue stained protein bands were detected in supernatant due to the low abundance.
- (e) *H. schachtii* susceptibility assay of Hs4E02E lines compared with the non-transformed Col-0. Asterisks indicate datasets significantly different according to paired *t*-tests ($n = 90$; $P < 0.05$).
- (f) Quantitative analysis of *B. cinerea* symptoms on *A. thaliana* transgenic and non-transformed Col-0 leaves. α , β , and γ indicate datasets significantly different according to one-way analysis of variance (ANOVA) followed by Tukey's tests ($n = 41$; $P < 0.001$). Lesion areas were measured 48 h after inoculation. Data points represent average lesion areas \pm SE. Similar results were obtained from three independent experiments.
- (g) *B. cinerea* susceptibility assay on leaves of Hs4E02E lines compared with the non-transformed Col-0.



As a first measure of detecting potential roles in defense modulation of Hs4E02, we assessed transcript levels of a panel of known defense-related plant genes in the Hs4E02E lines. For this aspect, we chose the general defense marker gene *MEKK1* (*MAPK/ERK kinase kinase member A1*), the marker genes of the salicylic acid signaling pathway *PAD4* (*Phytoalexin Deficient 4*), *EDS1* (*Enhanced Disease Susceptibility 1*), *WRKY40* (*WRKY DNA-binding protein 40*) and *PR1* (*Pathogenesis-Related 1*), as well as the jasmonate-responsive plant defensin gene *PDF1.2*. We assessed their expression in root tissues of non-infected Hs4E02E expressing lines in comparison with wild-type plants. While we observed significant upregulation (7- to 60-fold) of *PAD4* and *WRKY40* mRNAs in the Hs4E02E lines, we also detected a 17- to 23-fold downregulation of *PDF1.2* (Figure 1a), whereas the remaining genes did not show altered transcript levels. These findings confirm that Hs4E02 is likely to alter certain defense responses. Next, we analyzed whether the differential expression of these known defense genes is accompanied by changes in susceptibility to the sugar beet cyst nematode *H. schachtii*. Using our established nematode infection protocol (Baum *et al.*, 2000), we observed that the Hs4E02E transgenic lines were 22% more susceptible to the sugar beet cyst nematode compared with non-transformed control plants (Figure 1d), which supported the hypothesis that the Hs4E02 effector is a plant defense modulator. These observations also complemented previous data in which *in planta* expression of RNAi constructs targeting Hs4E02 in the infecting nematodes resulted in up to a 20% reduction in *H. schachtii* female numbers developed on RNAi roots (Patel *et al.*, 2008).

The observation in Hs4E02E transgenic lines of downregulation of *PDF1.2*, a protein whose upregulation is required for resistance to plant necrotrophic pathogens (Penninckx *et al.*, 2003), led us to question whether this alteration was accompanied by changes in susceptibility to necrotrophic pathogens. To answer this question, we assessed the susceptibility of *A. thaliana* Hs4E02E transgenic lines to the necrotrophic fungus *Botrytis cinerea*. When compared with the wild-type control, the local symptoms of fungal infection were significantly higher in Hs4E02E lines (Figure 1e,f), indicating Hs4E02 also modulates *A. thaliana* susceptibility to necrotrophic parasites.

These results led us to question whether Hs4E02 can activate or suppress general defense responses. To assess this possibility, we tested whether Hs4E02 can activate general stress-mediated responses by comparing callose deposition and reactive oxygen species (ROS) accumulation between uninfected Hs4E02E lines and uninfected non-transgenic *A. thaliana* control plants. Our comparative analyses did not show any significant difference between these treatments (Figure 1b). Next, we conducted an experiment to check if Hs4E02 can suppress plant innate immune responses in heterologous immunosuppression

assays. For this purpose, we transiently expressed Hs4E02 fused with a type III secretion system signal in non-pathogenic *Pseudomonas fluorescens* strain Effector-to-Host Analyzer (EtHAN) and pathogenic *Pseudomonas syringae* (*Pst*) strain DC3000 for basal immunity and hypersensitive cell death response (HR) suppression experiments, respectively (Chakravarthy *et al.*, 2009; Noon *et al.*, 2016). To assess the ability of this effector to suppress basal or PAMP-triggered immunity (PTI), we inoculated wild-type EtHAN or EtHAN that expressed *Hs4E02* into *Nicotiana benthamiana*, and the infiltrated sectors were then challenged with *Pst* DC3000. There were no incidences of HR in the overlapping zones, revealing that Hs4E02 does not suppress basal/PAMP-triggered plant immunity (Figure 1c). Similarly, to assess this effector's ability to suppress effector-triggered immunity (ETI), we infiltrated *N. benthamiana* leaves with either wild-type *Pst* DC3000 or with *Pst* DC3000 expressing *Hs4E02*. There was no significant HR suppression in zones infiltrated by *Pst* DC3000 expressing *Hs4E02* nor those infiltrated with non-transformed *Pst* DC3000. Therefore, Hs4E02 does not suppress ETI (Figure 1c).

The data presented above show that while Hs4E02 alters specific host defense pathways, it does not alter plant immunity on a global scale. While the expression of effectors in host plants can offer important insights into effector functions, this approach does not divulge mechanistic details. We therefore focused in the next steps on the effector's mode-of-action by identifying plant proteins targeted by Hs4E02.

Hs4E02 specifically interacts with the *A. thaliana* protease Resistant-to-Dehydration 21A (RD21A)

Previously, the soybean cyst nematode effector Hg4E02 was shown to contain a SV40-type NLS, and its functionality was confirmed experimentally by localizing Hg4E02 to the nuclei of onion epidermal cells and *A. thaliana* protoplasts (Elling *et al.*, 2007). The sugar beet cyst nematode effector Hs4E02 also contained an NLS and was predicted to be a nuclear effector. Similarly for Hg4E02, it also does not contain any apparent catalytic or DNA-binding domains. Therefore, we hypothesized that Hs4E02 interacts with and modulates host protein(s) with enzymatic or regulatory functions. We therefore conducted yeast two-hybrid analysis using the Hs4E02 protein without its signal peptide as bait to screen prey libraries developed from *H. schachtii*-infected *A. thaliana* roots (Hewezi *et al.*, 2008). The strongest interacting protein was 'Resistant-to-Dehydration 21A' (RD21A; *At1 g47128*), a PLCP, which was identified in 13 independent yeast clones. Sequencing the prey inserts in all 13 independent colonies revealed that they all coded different overlapping parts of the RD21A protein (Figure S2).

The interaction between Hs4E02 and RD21A is particularly interesting as it has been previously documented that

RD21A has a strong pro-death function, plays a key role in programmed cell death (PCD), and is targeted by pathogen effectors in other plant-pathosystems (Shindo *et al.*, 2012; Lampl *et al.*, 2013). Being obligate and sedentary biotrophs, cyst nematodes have to prevent PCD to maintain syncytium viability for relatively long time periods to complete their life cycles. Throughout this period, the threat exists that the host plant triggers PCD to terminate the feeding site and kill the cyst nematode, as observed in nematode-resistant sugar beet and soybean cultivars (Holtmann *et al.*, 2000; Mitchum, 2016). Therefore, local suppression of PCD in the developing syncytium of the host plant appears to be vital for the successful establishment of a feeding site. As a consequence, we hypothesized that Hs4E02 could be targeting RD21A to modulate its function and prevent or delay PCD. Our hypothesis was supported by data presented by Lozano-Torres *et al.* (2014) who showed that *A. thaliana* mutants lacking the PLCPs PAP1, PAP4, and PAP, and in particular RD21A, were more susceptible to *H. schachtii* infection. Additionally, the critical roles in plant immunity played by the orthologous members of RD21A in various plant species such as C14 from tomato and *N. benthamiana*, and CP1 from corn have also been documented (Misas-Villamil *et al.*, 2016). Therefore, we decided to examine this protein–protein interaction in detail.

Full-length RD21A comprises 462 amino acids and, starting at the N-terminus, contains a signal peptide, an autoinhibitory pro-domain, a protease domain, a proline-rich region, and a granulin domain (Yamada *et al.*, 2001; Gu *et al.*, 2012) (Figure 2a). This pre-protein undergoes extensive post-translational processing, the details of which are not yet clear. According to the available information, the autoinhibitory pro-domain, which prevents unintended activation of the protease, together with the signal peptide were proteolytically removed at the destination cellular compartment, therefore giving rise to an intermediate form of RD21A (iRD21A) (Gu *et al.*, 2012). iRD21A undergoes further maturation in which all the other domains are proteolytically cleaved to form the mature and active form of RD21A, or mRD21A, which consists of only the protease domain (Yamada *et al.*, 2001). The mRD21A isoform is located in the vacuole and is released into the apoplast under stress conditions (Hatsugai *et al.*, 2009).

When aligning the 13 RD21A prey yeast clones with the full-length RD21A cDNA, we observed that all clones shared an 85-amino acid stretch (R237-K321) that resides within the 216 residue-long cysteine protease catalytic domain (L137-I352, mRD21A) of the RD21A protein (Figure S2). Therefore, the effector Hs4E02 is likely to interact with RD21A close to, or at, the protease domain.

To confirm the specificity of this interaction, we cloned a truncated form of RD21A that only contained this protease

domain (mRD21A) into the yeast prey vector pGBKT7 and co-transformed yeast cells with the bait vector expressing Hs4E02 and the prey vector expressing mRD21A. As negative controls, cells were transformed with the mRD21A construct with either the empty bait vector or the bait vector containing a human Lamin C coding sequence (Clontech, Takara Bio USA, Inc., CA, USA). Strong yeast colony growth on selective medium was observed only for yeast cells transformed with mRD21A and Hs4E02, while negative controls did not grow (Figure 2b). These data confirmed a specific interaction between Hs4E02 and the protease domain of RD21A within yeast cells.

As a confirmation of the physical interaction between Hs4E02 and RD21A, we conducted *in vitro* co-immunoprecipitation assays. We used *Escherichia coli* strain BL21 to express Hs4E02 and mRD21A proteins fused at their N-termini with His and HA tags, respectively (Figure 2c,d). HA-mRD21A was purified on Ni-NTA resin from crude protein extract only in the presence of His-Hs4E02, confirming a strong *in vitro* interaction between the effector and this plant protein.

RD21A is differentially expressed in infected roots and developing syncytia

As we confirmed that Hs4E02 targets RD21A, which participates in plant responses to pathogen attacks, we examined RD21A expression in *A. thaliana* root tissue, particularly during nematode infection. First, we quantified RD21A mRNA abundance in root tissues of *H. schachtii*-infected and mock-infected wild-type plants at 7 days post-inoculation. Data from three independent biological experiments revealed that RD21A mRNA abundance increased five-fold in nematode-infected roots (Figure 3a). Interestingly, Hs4E02 expression in transgenic *A. thaliana* lines did not affect RD21A expression levels by itself in uninfected tissues (Figure 3b).

To investigate whether the RD21A gene is expressed at the site of nematode infection, we developed transgenic *A. thaliana* lines expressing the beta-glucuronidase (GUS) reporter gene *uidA* driven by the promoter of RD21A. While uninfected roots of RD21A-promoter:GUS transgenic plants did not exhibit any visually detectable GUS expression in our X-gal assessments (Figure 3c), a strong and specific induction of GUS activity in the early syncytium (4 DPI) was detected (Figure 3d). After this initial promoter activation, GUS activity in the syncytium then gradually decreased in the later stages of nematode development, while strong activation of GUS expression became evident in regions flanking the infection sites (Figure 3e,f). We concluded that RD21A is expressed in infected *A. thaliana* roots and in the developing syncytium where it, therefore, can be targeted by Hs4E02.

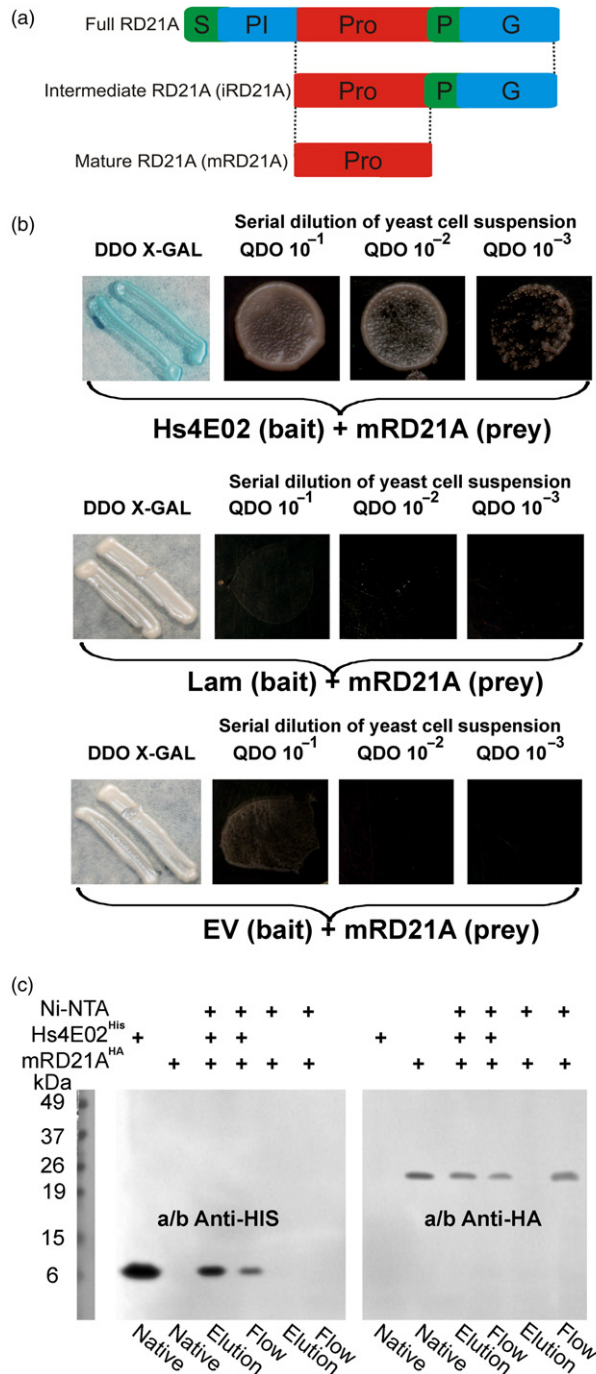


Figure 2. Hs4E02 specifically interacts with RD21A.

(a) Schematic representation of the RD21A protein. S – vacuole-targeting signal peptide, PI – autoinhibitory pro-domain, Pro – protease domain, P – proline-rich region, G – granulin domain.

(b) Interaction between Hs4E02 (bait) and mRD21A (prey) in yeast (*Saccharomyces cerevisiae* strain AH109) was visualized by α -galactosidase activity (blue color, X-GAL) on non-selective medium DDO (SD/-Leu/-Trp/ α -Gal) and by differential growth on the selective synthetic dropout (SD/-Leu/-Trp/-Ade/-His) medium (QDO) at three culture concentrations 10^{-1} , 10^{-2} , 10^{-3} . Yeast cells containing the RD21A^P prey plasmid along with either the empty bait vector (EB) or the bait vector containing the human *Lamin C* gene (Lam) fail to grow on the selective medium or to produce α -galactosidase activity beyond the background level.

(c) Western blot analysis for pull-down assay. Hs4E02 protein fused with HIS-tag on N-terminus and mRD21A fused with HA-tag on N-terminus were used. Input bands represent the expressed proteins. Flow fraction – proteins left in liquid phase after incubation with Ni-NTA; eluate – protein sample eluted from Ni-agarose (Ni-NTA).

independently to re-confirm these results (Figure 4a). For this *in planta* assay, we chose to express the intermediate isoform iRD21A because this is the predominant and most stable isoform that appears in the destination cellular compartment (vacuole) and then slowly gets proteolytically processed into the mature form, mRD21A (Yamada *et al.*, 2001; Gu *et al.*, 2012). The RD21A–YFP fusion protein produced a fluorescence signal similar to the appearance of vacuolar-targeted GFP reported by Tamura *et al.* (2003), while Hs4E02 showed a strong nuclear localization. These data raised the question how these potentially interacting partners interact *in planta* if they accumulate in distinct cellular compartments.

To address this question, first we used bimolecular fluorescence complementation (BiFC, Ghosh *et al.*, 2000) as an *in planta* assay to further scrutinize this interaction, as this method would also reveal the cellular compartment in which the interaction is taking place. Our BiFC assay showed strong fluorescence (Figure 4a), confirming the physical interaction between Hs4E02 and iRD21A. Interestingly, we observed that this interaction occurred in the cytoplasm and the nucleus, two cellular compartments that have not been reported for RD21A (Figure 4a). We also performed another BiFC assay using the unrelated *A. thaliana* protein, DJ-1 in combination with Hs4E02 to confirm that the effector interaction with RD21A is specific. We chose the DJ-1 protein as a negative control because it was reported to be localized in both the cytoplasm and nucleus (Xu *et al.*, 2010). The lack of any fluorescence signal from this control assay indicated that Hs4E02 specifically targeted RD21A, and that the interaction was taking place in the nucleus and cytoplasm.

One explanation for the strong nucleo-cytoplasmic signals of the Hs4E02-RD21A interaction could be that there is a small, undetected fraction of RD21A always present in the nucleus and cytoplasm. However, the RD21A-fluorescent protein fusion studies performed by our group and reported earlier (Yamada *et al.*, 2001; Lampl *et al.*, 2013)

Hs4E02 induces re-localization of RD21A

Hs4E02 was predicted to accumulate in the plant nucleus due to the presence of the NLS, whereas RD21A accumulates in entirely different cell compartments, i.e. the vacuole and endoplasmic reticulum (ER-bodies) as previously reported (Hayashi *et al.*, 2001; Yamada *et al.*, 2001). We transiently expressed the intermediate isoform of RD21A (iRD21A) as well as Hs4E02 C-terminally fused to the yellow fluorescent protein (YFP) in *N. benthamiana*

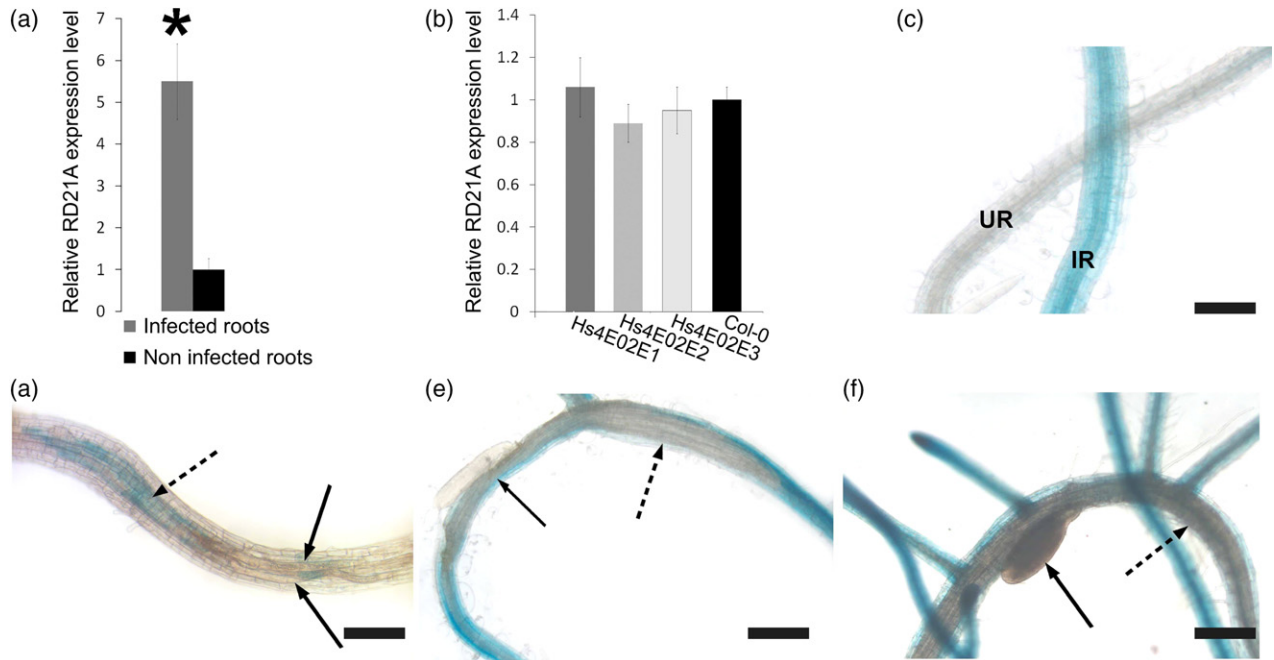


Figure 3. *RD21A* expression levels change in response to *Heterodera schachtii* infection.

(a) qRT-PCR analysis comparing *RD21A* expression in *Col-0* roots under non-infected and *H. schachtii*-infected conditions. Mean values of three independent biological replicates significantly different ($P < 0.05$) from controls as determined by paired *t*-test are denoted by asterisks. (b) qRT-PCR expression analysis of *RD21A* in *Hs4E02E* non-infected lines. Each bar represents mean value of three independent biological replicates. (c–f) Histochemical localization of GUS activity driven by the *RD21A* promoter in transgenic *A. thaliana* seedlings and in response to *H. schachtii* infection. (c) The uninfected (UR) and infected (IR) roots at 14 DPI, (d) roots infected with *H. schachtii* at the J2 development stage, (e) at the J3 stage, and (f) at the J4 stage. Solid black arrows point toward nematodes, dashed arrows point toward syncytia. Bars = 100 μm .

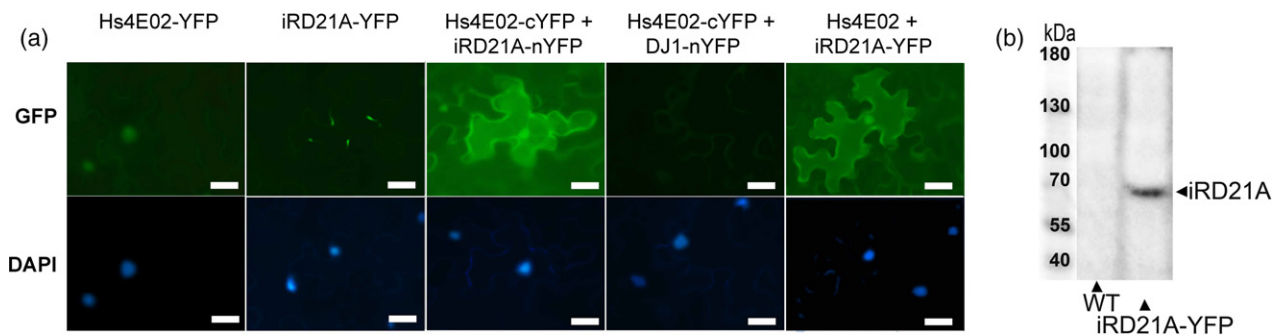


Figure 4. *Hs4E02* induces re-localization of *RD21A*.

(a) *In planta* subcellular localization of *Hs4E02* and *RD21A* (Columns 1, 2 and 5). The coding sequences of *Hs4E02* and *iRD21A* were fused with YFP. *Hs4E02* showed nuclear accumulation (first column) while *iRD21A* showed a characteristic ‘speckled’ accumulation (second column). Nuclear-cytoplasmic fluorescence produced by *iRD21A*-YFP fusion construct in the presence of *Hs4E02* validate effector-induced re-localization of *RD21A* (fifth column). BiFC visualization of the *Hs4E02* and *RD21A* interaction (column 3 and 4). Leaf sectors co-expressing *Hs4E02*-cYFP and *iRD21A*-nYFP constructs showed strong fluorescence in cytoplasm and nucleus (fourth column), while the absence of fluorescence in the leaf sectors co-expressing *Hs4E02*-cYFP and the coding sequence of an unrelated protein *AtDJ1* fused with nYFP confirmed the specificity of the *Hs4E02* and *RD21A* interaction. Both assays were conducted in *Nicotiana benthamiana* leaves infiltrated with *Agrobacterium tumefaciens* GV3101 cells harboring expression constructs. Images were taken with a fluorescence microscope at 4 DPI. All fluorescent images were taken under consistent parameters: shutter, exposure time and UV intensity. Images were taken using a GFP filter (upper row) and a DAPI filter (lower row) to visualize nuclei stained with DNA-specific stain. Bar = 10 μm .

(b) Western blot analysis of the total soluble protein from *RD21A*-YFP and *Hs4E02* co-infiltrated into *N. benthamiana* leaves. Protein was detected with anti-YFP monoclonal antibody. The observed band of approximately 64 kDa confirms expression of the intermediate form of the *RD21A* protein fused with YFP (approximately 38 kDa + 26 kDa). WT – non-infiltrated *N. benthamiana* control leaves.

were not able to document any *RD21A* presence in these compartments, and this explanation therefore seems unlikely. A more likely explanation is that *Hs4E02* changes the

subcellular localization of *RD21A*. To investigate this hypothesis, we co-expressed a *iRD21A*-YFP fusion construct with the unlabeled *Hs4E02* coding sequence in *N.*

benthamiana. We combined both gene constructs into a single binary vector (pPZP-RCS2; Chung *et al.*, 2005) to ensure simultaneous expression of both gene constructs in all transformed cells. Interestingly, we observed the strong nucleo-cytoplasmic fluorescence of the RD21A–YFP fusion (Figure 4a). To discern whether the observed fluorescence signals are from RD21A fusions and not from free YFP that could have been cleaved *in planta*, western blot analysis of fluorescing leaf tissues was performed (Figure 4b). This experiment showed only the band size expected for the intact fusion protein, indicating that the observed fluorescence is representative of RD21A distribution. Collectively, our data indicated that the Hs4E02 effector not only binds to RD21A *in vivo* but also causes this protease to accumulate in different cell compartments.

Activity-based protein profiling reveals no suppression of RD21A activity in the presence of Hs4E02

Because we observed and confirmed the binding of the Hs4E02 effector to RD21A in or around the protease active site, we examined if this interaction affected the enzymatic activity of the RD21A protease using activity-based protein profiling (ABPP). ABPP is an effective method for the identification, functional characterization and annotation of enzyme activities in cell extracts and living cells (Cravatt *et al.*, 2008; Edgington *et al.*, 2009). ABPP is based on the

design of biotinylated or fluorescent active-site-directed small molecules (probes) that bind covalently to the active site residues of enzymes in complex proteomes. Therefore, this method gathers information about the functional state of enzymes rather than about their abundance.

To determine any altered activity of RD21A in the presence of the Hs4E02 effector, root sections of wild-type *Col-0* and Hs4E02E plants were collected at 4 weeks post-germination, and the extracted soluble proteins were labeled with fluorescent activity-based probes. For the analysis of specific RD21A activity, we used activity probe MV201 (Verdoes *et al.*, 2006), which is based on vinyl-sulfone reactive groups and has been used specifically to analyze activities of the PLCPs (Gu *et al.*, 2010). Previous western blot studies revealed that there are two detectable RD21A isoforms in crude plant protein extracts. One is the 40 kDa intermediate isoform (iRD21A) consisting of protease, proline-rich, and granulin domains, and the other is the 30 kDa mature isoform (mRD21A) consisting of the protease domain and probably a partial proline-rich domain (Yamada *et al.*, 2001; Kaschani *et al.*, 2009; Gu *et al.*, 2010).

As shown in Figure 5(a,b), labeling of protein extracts from root sections of Hs4E02E plants was not different from the signals obtained for wild-type root sections. Both assays showed activity bands corresponding to the two

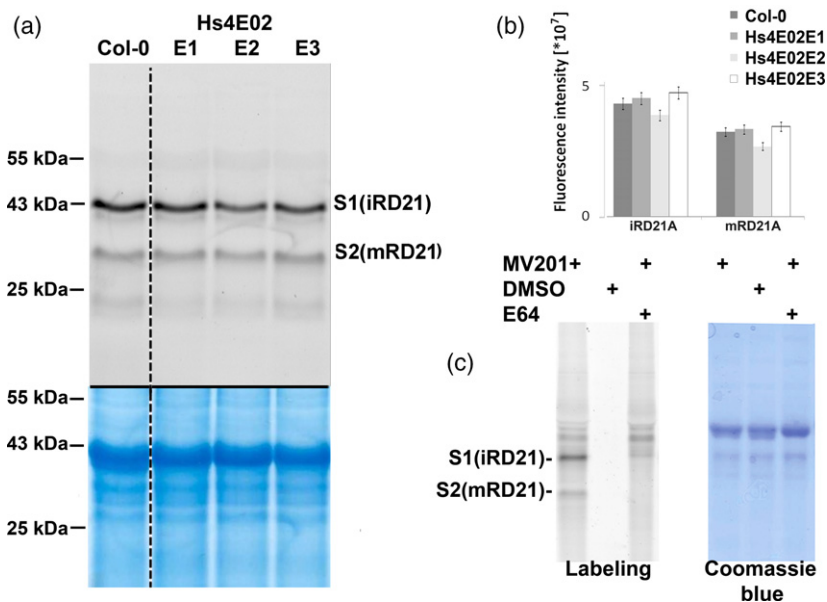


Figure 5. Hs4E02 does not inhibit RD21A activity.

(a) Comparative labeling of PLCPs in the leaves of non-infected *Hs4E02E* lines with MV201. Leaf extracts of equal fresh weights were labeled for 5 h with 2 μ M MV201 at pH 4.5, and fluorescently labeled proteins were detected by scanning. Experiment was repeated in three biological replicates (E1, E2, E3) and blue color gels represent staining of total protein with Coomassie blue, which was used as a control to show equal amount of protein in samples.

(b) Quantification of fluorescence intensity of gel signals S1 and S2 from 5A. No significant differences to the control were detected in three independent biological samples (*t*-test; $P < 0.05$).

(c) Signals are blocked by pre-incubation with PLCP inhibitor E64. A mix of leaf extracts shown in Figure 5(a) was pre-incubated with and without E64 and then labeled with and without MV201. Labeled proteins were detected in protein gel by fluorescent scanning.

Table 1 List of identified and confirmed interactors of RD21A (www.arabidopsis.org)

Gene locus	Gene ID	Brief description	Predicted subcellular localization	Predicted function
AT4G28250	ATEXPB3	Expansin B3	Apoplast/cell wall	Cell wall organization, syncytium formation, unidimensional cell growth
AT5G10560	ATXYL	1,4-beta-xylosidase	Apoplast/cell wall/ cytoplasm	Carbohydrate metabolic process
AT1G26630	ATELF5A-2	Eukaryotic elongation factor 5A-2	Cytoplasm	Pathogen-induced cell death in Arabidopsis
AT5G67360	SBT1.7	Subtilase family protein	Apoplast/cell wall	Serine-type endopeptidase is indirectly involved in the rapid rupture of the outer wall in seeds
AT3G23490	CYN	Cyanate hydratase	Cytoplasm	Cyanate catabolic and metabolic process, response to salt stress
AT1G13440	GAPC2	Glyceraldehyde-3-phosphate dehydrogenase C-2	Apoplast/cell wall/ cytoplasm	Transduce hydrogen peroxide signals in the Arabidopsis response to stress
AT5G13980	GlyH	Glycosyl hydrolase family 38 (alpha-mannosidase)	Cytoplasm/ apoplast/cell wall	Glycosylation of proteins via mannose metabolic process
AT2G39310	JAL22	Jacalin-related lectin 22	Cytoplasm	Carbohydrate (mannose)-binding function, first-line defense against invading microorganisms

RD21A isoforms iRD21A and mRD21A. In order to discern that the obtained labeling is truly due to protease function, we used the E64 cysteine protease inhibitor to pre-incubate samples (Hanada *et al.*, 1978). This treatment prevented subsequent activity labeling (Figure 5c), which further confirmed that the observed 30 and 40 kDa bands represented active forms of RD21A. Therefore, our results indicated that even though Hs4E02 strongly interacted with and re-localized the RD21A protease, it did not alter the enzymatic activity of RD21A. We therefore concluded that the effector causes re-localization of the RD21A protease in its active form. It is plausible that by changing the location of the RD21A protease, it is removed from its usual substrate, this disrupts the enzyme's pro-death function. In addition, RD21A in its new location might target a different set of substrates manifesting a different function. These results suggest that the parasitic strategy of the nematode is to interfere with normal, presumably defense-related, RD21A function using the effector Hs4E02, but also to use the re-localized RD21A protease for a different, yet to be identified, novel purpose.

RD21A interacts with multiple stress and carbohydrate metabolism-related proteins in yeast two-hybrid assays

No RD21A substrates have been identified to date, this hampers understanding the enzyme's functional relevance in general and specifically during nematode infection. We therefore proceeded to identify potential RD21A substrates that could pinpoint the cellular networks that this protease modulates. To identify potential targets of RD21A, we performed yeast two-hybrid analyses using only the protease domain of RD21A in the bait vector. In screens using the wild-type protease domain sequence, very few yeast colonies were recovered, most likely this was due to the

proteolytic activity of the protease domain. To prevent potential target protein degradation through the proteolytic activity of the protease domain during protein interactions, we generated a mutated inactive version of RD21A. For this, we used i-Tasser prediction software (<http://zhanglab.ccmb.med.umich.edu/I-TASSER/>) to identify the critical cysteine residue (C161) likely to be involved in the proteolysis reaction and mutated this cysteine residue to alanine. We then cloned the resultant construct in the bait vector. Using this mutated clone, we were able to obtain yeast colonies on selective medium. Targeted co-transformation of the identified candidate RD21A-interactors resulted in the identification of eight interacting proteins. Interestingly, all interacting proteins had predicted or confirmed functions in either stress response, cell wall biology or carbohydrate metabolism (Table 1 and Figure S3). One of the interacting proteins, AtEXPB3, was shown to be strongly upregulated in syncytia induced by *H. schachtii* (Wieczorek *et al.*, 2006).

Further in-depth analysis will be needed to confirm RD21A interaction with the predicted interacting proteins *in planta*. However, our preliminary data supported our earlier findings of altered defense gene expression and pathogen susceptibility as a function of Hs4E02. The finding of the four interacting proteins that are involved in either control of cell wall composition or carbohydrate metabolism was unexpected. Therefore, we analyzed cell wall composition of Hs4E02E lines. We compared the root cell wall monosaccharide composition of Hs4E02E plants with control non-transformed plants, and the results demonstrated significant differences in their composition. In comparison with the wild-type, root cell walls of Hs4E02E plants contained higher amounts of mannose (28%) and glucuronic acid (57%) (Table 2), indicating that

Table 2 Monosaccharide composition (mol%) of the cell wall from roots of Hs4E02E lines and Col-0

	Fuc	Rha	Ara	Gal	Glu	Xyl	Man	GalA	GluA
Hs4E02E	4.88 ± 0.61	5.98 ± 2.65	21.43 ± 4.20	30.53 ± 7.07	16.52 ± 3.21	16.27 ± 2.22	3.42 ± 0.19 ^a	2.22 ± 0.70	0.74 ± 0.08 ^a
Col-0	4.21 ± 0.73	5.77 ± 0.71	20.84 ± 1.16	30.27 ± 3.05	22.32 ± 3.44	15.88 ± 3.73	2.67 ± 0.55	1.57 ± 0.17	0.47 ± 0.18

^aSignificantly different (*t*-test, *P* < 0.01, *n* = 3).

altered cell wall architecture could be a pleiotropic effect of the effector Hs4E02.

DISCUSSION

Cyst nematodes are sedentary obligatory biotrophic parasites that rely solely on specialized feeding structures, the syncytia, for their nutritional requirements. Host plants, conversely, upregulate defense responses during nematode infection and trigger PCD to prevent syncytia and starve nematodes during resistant interactions (Holtmann *et al.*, 2000; Kandoth *et al.*, 2011; Liu *et al.*, 2011; Siddique *et al.*, 2014). Therefore, cyst nematodes have to orchestrate robust and sustained suppression of host defenses to maintain syncytial viability. Plants possess large arsenals of receptor molecules that recognize a wide array of molecular patterns and effectors produced by a broad range of pathogens (Smakowska-Luzan *et al.*, 2018). Recognition triggers activation of highly interconnected intracellular signal transduction pathways, which ultimately culminates with the activation of local and systemic defense responses and PCD (Jones and Dangl, 2006; Biere and Govere, 2016). To quench such highly interconnected defense networks, cyst nematodes must possess strategies and deploy effectors that target multiple host components or target a component that has the potential to interact with and modulate the activities of multiple host components of the signaling networks. Conducting in-depth functional characterization of effectors can reveal such novel strategies and help to build the entire interactome of effectors for a particular parasite and its host.

In this study, we conducted functional characterization of cyst nematode effector Hs4E02 and discovered a strategy adapted by cyst nematodes to modulate the plant defense network. Our results show that Hs4E02 targets the PLCP RD21A, which possesses a pro-death function.

It is established that PLCPs play key roles in plant immunity. First, multiple studies have reported altered susceptibility of mutant plants expressing altered levels of PLCPs to various pathogens. These studies showed that the members of this protease family from *A. thaliana*, tomato and *N. benthamiana* are involved in molecular plant interactions with a broad range of pathogens such as the pathogenic fungi *B. cinerea*, *Cladosporium fulvum*, *Colletotrichum destructivum*, and *Sclerotinia sclerotiorum*, the pathogenic bacteria *Ralstonia solanacearum* and *P. syringae*, the oomycete *Phytophthora infestans*, and the

nematode *H. schachtii* (Dixon *et al.*, 2000; Bernoux *et al.*, 2008; Lozano-Torres *et al.*, 2012; Shindo *et al.*, 2012; Lampl *et al.*, 2013).

Second, the critical roles played by PLCPs in plant immunity are highlighted by reports describing effectors deployed by different pathogens to directly target these proteases to modulate their activities. A recent study showed that an effector protein (Mc1194) secreted by the root-knot nematode *Meloidogyne chitwoodi* interacts with RD21A in *A. thaliana* (Davies *et al.*, 2015). The RD21 ortholog C14 from tomato is targeted by the effectors Avrblb2, EpiC1 and EpiC2 secreted by *P. infestans*, which enhances susceptibility of host plants (Kaschani *et al.*, 2010; Bozkurt *et al.*, 2011; Misas-Villamil *et al.*, 2016). Maize PLCPs CP1A, CP1B, XCP2 and CP2 are targeted by the effector Pit2 secreted by the fungal pathogen *Ustilago maydis*, which leads to the inhibition of salicylic acid-associated plant defense (Mueller *et al.*, 2013). Another member of this class of proteases – CYP1 from tomato – is targeted by an effector of the tomato yellow leaf curl geminivirus to suppress hypersensitive response reactions (Bar-Ziv *et al.*, 2012). Similarly, PLCP RD19 is targeted by the effector protein PopP2 from *R. solanacearum* (Bernoux *et al.*, 2008). Taken together, these reports confirmed that PLCPs are major players in host–parasite interactions and that pathogens have evolved specific effectors that target these proteases to modulate their functions.

The role of RD21A previously has been investigated in plant–cyst nematode interactions. Lozano-Torres and co-authors have shown that *A. thaliana* RD21A knockout mutant lines are more susceptible to cyst nematode infection (Lozano-Torres *et al.*, 2012), suggesting that RD21A plays an important role in resisting nematode infection. Another study that compared gene expression profiles of developing syncytia in soybean near-isogenic lines differing at the *Rhg1* (for Resistance to *H. glycines*) locus, showed that expression of the RD21A soybean homologue was significantly upregulated in a resistant line (Kandoth *et al.*, 2011). This evidence is especially significant because this particular soybean line resists cyst nematode infection by inducing PCD at the sites of infection, thereby abolishing syncytia. In addition, RD21A previously has been shown to have a ‘pro-death function’ (Lampl *et al.*, 2013). Our mRNA steady-state analyses as well as promoter data also showed that, in response to nematode attack, *A. thaliana* plants upregulate RD21A expression, at least, at the early stages

of infection. All these results indicate that RD21A plays a key role in plant–nematode interactions that it can negatively affect nematode parasitism, and that plants upregulate its expression as a part of their defense response against nematode attack. Hence, nematodes must counteract this response to establish successful infection.

Although according to our data, *RD21A* expression decreases during the later developmental stages of cyst nematode infection, it has been reported that PLCPs are stable proteins that can stay active for long times after translation (Richau *et al.*, 2012). It appears that cyst nematodes need to devise a strategy to specifically address existing RD21A protein that was synthesized during the early stages of nematode infection. Based on our results, we propose that cyst nematodes deploy effector Hs4E02 to target the RD21A protein and modulate its functionality.

One of the possible strategies to modulate enzyme functionality is to inactivate it. Our yeast two-hybrid data indicated that the effector Hs4E02 interacts specifically with the catalytic domain of RD21A, which would suggest such a possibility. However, we demonstrated that the enzymatic activity of RD21A was not affected and that instead of inactivating the protease, Hs4E02 causes a re-localization of RD21A from its known site of defense-related activity. There is a possibility that Hs4E02 binds to and inhibits other PLCP homologues as well. However, it is important to note that while we discovered 13 independent clones of RD21A, we did not identify any clone from either of its homologues from our yeast two-hybrid assay.

As it was mentioned above, RD21A is a vacuolar protease, which is released into the apoplast under stress conditions (Hatsugai *et al.*, 2009). Our co-localization data show that its subcellular localization changes to the nucleus and cytoplasm in the presence of the effector. This means that the effector ‘mis’-localizes the protease from its usual environment, therefore most likely preventing it from performing its defense roles. In addition, this ‘mis’-localization introduces RD21A in an active form to a new environment, thereby inducing additional, so far unknown, effects on host cells. This seems an effective strategy as it removes a protease from one set of substrates and exposes it to novel proteins, which otherwise might not be accessible to the protease. In other words, one set of actions is inhibited, but, most likely, completely different cellular pathways are initiated as a result of this strategy. In the case of RD21A, which normally is released into the apoplast to trigger a hypersensitive response to pathogen invasion (Hatsugai *et al.*, 2009), its re-localization could prevent degradation of the intended target proteins within the extracellular space. Conversely, the new localization in the cytoplasm/nucleus could have consequences that so far remain unknown.

The interaction and re-targeting between a nuclear effector and a vacuolar protein was reported before for vacuole-localized paralog RD19, which is targeted by the

effector protein PopP2 from *R. solanacearum*. Similar to RD19, the precise mechanism behind the effector-mediated re-localization of RD21A remains unresolved. However, there are several important differences between RD19 and RD21A in these two pathosystems. While the RD19-PopP2 complex is re-localized to the plant nucleus (Bernoux *et al.*, 2008), it was not investigated if this particular PLCP activity was inhibited by the effector. Furthermore, the same study demonstrated that RD19 is not an essential component of the basal plant defense mechanisms and, therefore, the functional relevance of this re-localization remains unclear.

Although somewhat premature, the altered monosaccharide composition as a function of effector expression is interesting. The effector-expressing lines revealed higher amounts of mannose (28%) and glucuronic acid (57%), which both are part of cell wall hemicellulose polysaccharides (Burton *et al.*, 2010; Scheller and Ulvskov, 2010). These results could indicate an increase in cell wall hemicellulose content or branching in response to Hs4E02E. Alteration of polysaccharide composition or increase of their branching can affect the cell wall mechanical properties adjusting its flexibility/rigidity, which could impact syncytium development and expansion. Perhaps, modulation of cell wall properties via cell wall-modifying enzymes is one of the new RD21A functions after its re-localization by Hs4E02. In fact, alteration of plant cell walls by an effector was previously shown to affect nematode infection success (Hewezi *et al.*, 2008). In addition, the roles of glucuronic acid in cyst nematode infection recently have been characterized. *A. thaliana* mutants defective in UDP-glucuronic acid synthesis were less susceptible to *H. schachtii* infection and showed smaller syncytia (Siddique *et al.*, 2012).

In summary, our functional characterization of the effector Hs4E02 has revealed an evolutionary advanced strategy of cyst nematodes. We show that this effector specifically targets the important pro-death PLCP RD21A and, unlike other cyst nematode effectors that modulate the activities of their interacting host components, Hs4E02 achieves its virulence function by altering the subcellular localization of this host protein in its active form, thereby maximizing the utility of a single effector.

EXPERIMENTAL PROCEDURES

Constitutive expression of *Hs4E02* in *A. thaliana*

The *Hs4E02* coding sequence was amplified without the signal peptide sequence using specific primers (Table S1) containing the restriction sites *Bam*HI and *Sac*I on the forward (*Hs4E02*-Af) and reverse primers (*Hs4E02*-Ar), respectively, for directional cloning into the pB1121 binary vector. This created a T-DNA cassette containing the *Hs4E02* coding sequence under the control of the *CaMV35S* promoter. The construct was transformed into *Agrobacterium tumefaciens* strain GV3101 using the freeze–thaw method

(An *et al.*, 1988). The resultant strain was used to transform *A. thaliana* ecotype *Columbia-0* using the floral dip method (Clough and Bent, 1998).

Quantitative RT-PCR analysis of *Hs4E02* lines

Total RNA was extracted from 5-week-old plants using the SV Total RNA Isolation kit (Promega, Madison, WI, USA), and cDNA synthesis was performed with the SuperScript III First Strand Synthesis system (Invitrogen, Thermo Fisher Scientific, Waltham, MA, USA) following the manufacturer's instructions. At least three separate biological replicates were used for each experiment. PCR reactions were run with the use of the Maxima SYBR Green qPCR Master Mix (2 \times ; Fermentas, Thermo Fisher Scientific, Waltham, MA, USA) in an I-Cycler (Bio-Rad, CA, USA) using the following program: 50°C-10', 95°C-5', and 40 cycles of 95°C-30" and 56°C-30" using gene-specific primers (Table S1). Expression levels of the gene-of-interest were calculated using the $2^{-\Delta\Delta CT}$ method (Livak and Schmittgen, 2001). The baseline was calculated using the *Hs4E02* expression level in the lowest expressing line.

Nematode assays

A nematode infection assay of *Hs4E02*-expressing *A. thaliana* lines was performed as previously described (Baum *et al.*, 2000). Inoculated plants were grown for 3 weeks, after which each inoculated plant was scored for the number of adult female nematodes. *P*-values for the difference in the average number of adult females between *Hs4E02*-expressing lines and the wild-type were calculated using a least squares mean model (nematode = plate genotype) (SAS).

Yeast two-hybrid assay and co-transformation validation

Yeast two-hybrid screening was performed as described in the BD Matchmaker Library Construction and Screening Kits (Clontech). The *Hs4E02* coding sequence was amplified without the signal peptide using specific primers (Hs4E02-Yf and Hs4E02-Yr) containing the restriction sites *EcoRI* and *PstI* and cloned into pGBKT7 bait vector to produce a fusion construct of *Hs4E02* and the GAL4 DNA-binding domain (BD). This construct was transformed into *Saccharomyces cerevisiae* strain Y187 to create the bait strain, which was mated separately with the three prey libraries (Hewezi *et al.*, 2008) in the compatible *S. cerevisiae* strain AH109. Screening and subsequent co-transformation analysis of interacting prey vectors was carried out according to Clontech protocols.

To validate protein–protein interaction between the effector protein and RD21A, the DNA sequence coding for the protease domain of the RD21A was amplified via PCR with the use of RD21A-Yf and RD21A-Yr primers.

Developing bait strain with mutant version of RD21A for yeast two-hybrid analysis

To develop the bait vector expressing an inactive form of RD21A, the nucleotide sequence coding for the protease domain was PCR-amplified as two parts using RD21Ce-F/RD21cmM-R and RD21Ce-R/RD21cmM-F primer pairs. The internal primer pair RD21cmM-F/RD21cmM-R was designed to substitute nucleotides CA to GC resulting in an amino acid change from Histidine to Alanine (marked as lower case bold letters in the primer sequences performed in Table S1). The resultant PCR product was diluted fourfold and used as a template for PCR amplification with RD21Ce-F and RD21Ce-R primers with an additional step of incubation at 72°C for 10 min before the first denaturation step. The resultant

PCR product was digested with appropriate enzymes and cloned into yeast bait vector pGBKT7.

In vivo bimolecular fluorescence complementation and colocalization assays

The nucleotide sequences coding for *Hs4E02* and the intermediate form of RD21A were amplified using corresponding primer pairs (Hs4E02-Tf/Hs4E02-Tr; RD21A-Tf/RD21A-Tr) containing restriction sites *EcoRI* and *BamHI* and high-fidelity proofreading Encyclo Polymerase (Evrogen.com). Obtained blunt PCR fragments were purified from the reaction mixture with the Silica powder kit (Invitrogen) and T-tailed by GoTaq (Promega) polymerase (incubated at 72°C for 10 min) and cloned into the pGEM-T Easy vector (Promega). Recombinant plasmids containing coding sequences were treated with corresponding restriction enzymes and obtained sequences were subcloned into pSAT4-cEYFP-C1 and pSAT4-cEYFP-N1 (*Hs4E02*), and pSAT6-nEYFP-C1 and pSAT 6-nEYFP-N1 (RD21A), and also pSAT6-EYFP-C1 resulting in expression constructs containing genes fused with the N- or C-terminus of the partial YFP sequence or N-termini of the full-length YFP. *Hs4E02*-cEYFP and RD21A-nEYFP were digested from pSAT plasmids using *I-SceI* (for pSAT4) and *PI-PspI* (for pSAT6) restriction enzymes and ligated to single binary vector pPZP-RCS2 (Chung *et al.*, 2005) sequentially digested with *I-SceI* and *PI-PspI*.

A nucleocytoplasmic At-DJ1a (*At3 g14990*) protein (Xu *et al.*, 2010) was used as a negative control to confirm the specificity of the BiFC. *Agrobacterium tumefaciens* cells harboring each construct were delivered to *N. benthamiana* leaves using the infiltration method described previously (Pogorelko *et al.*, 2014).

For co-localization assays, RD21A-YFP construct was co-infiltrated with *Hs4E02* expression construct, and after microscope observation, 6–8 leaf discs (5 mm diameter) were subjected for total protein extraction. Ground in liquid nitrogen, leaf samples were diluted with 50 μ L extraction buffer and centrifuged 15 000 *g* for 5 min at +10°C. Supernatant was used for western blot analysis.

In vitro protein expression and pull-down assay

The N-terminal His-tagged truncated *Hs4E02* lacking the secretion signal coding sequence was prepared by amplification of cDNA and cloning into the pET-15b vector (Novagen) containing an N-terminal 6xHis tag using gene-specific forward and reverse primers (Hs4E02-Ef and Hs4E02-Er). The N-terminally HA-tagged RD21A was constructed by replacing the N-terminal 6xHis tag sequence from the pET-15b vector with the HA-sequence, and fusing it with RD21A coding nucleotide sequence using primer pair RD21A-Ef/RD21A-Er.

The resultant pET-15b recombinant plasmids were subjected to pull-down assays according to the procedure described previously (Pogorelko *et al.*, 2016a,b).

In vivo RD21A promoter analysis

The promoter sequence of the RD21A gene (approximately 2 kb upstream of start codon) was amplified from *A. thaliana Columbia-0* using specific primers RD21AprF and RD21AprR and cloned into binary vector pBI101 and subsequently transformed first into *A. tumefaciens* cells and then to *A. thaliana* plants as described above.

The histochemical localization of GUS activity was performed as described previously (Jefferson *et al.*, 1987) with minor modifications. Plant leaf samples were immersed in a histochemical reaction mixture containing 1 mg mL⁻¹ X-Gluc (5-bromo-4-chloro-3-indolyl- β -D-glucuronide; Duchefa) in 150 mM potassium phosphate buffer pH 7.0, 10 mM potassium ferrocyanide, and 0.05% Triton X-100. The

histochemical reaction was performed in the dark at 37°C for 24 h. Tissue samples were viewed using a Zeiss SV-11 microscope, and the images were captured using a Zeiss AxioCam MRC5 digital camera and then processed using Zeiss Axiovision software (release 4.8).

Cell wall composition analysis

Cell walls were isolated from the plant tissue as described by Zabolina *et al.* (2008). Analysis of monosaccharide composition of cell walls was performed as described (Pogorelko *et al.*, 2011).

Determination of callose deposition and reactive oxygen species accumulation

Examination of callose deposition and ROS visualization were performed as described (Pogorelko *et al.*, 2013; Reem *et al.*, 2016).

PTI and ETI suppression assays

Hs4E02 was cloned into pEDV6 vector and transformed into *Pseudomonas* strains followed by standard infection assays as described previously for HgGLAND18 (Noon *et al.*, 2016).

Protein secretion

Accumulation of AvrRPS4:HA:Hs4E02 in *Pseudomonas* sp. and its secretion by the type III secretion system was verified according to Fabro *et al.* (2011). Pellet and supernatant fractions were analyzed by sodium dodecyl sulfate polyacrylamide gel electrophoresis (SDS-PAGE) and subjected to western blotting.

Western blots

Protein samples were analyzed by immunoblotting with tag-specific antibodies as described previously (Pogorelko *et al.*, 2016a,b). Primary anti-GFP monoclonal antibody (Covance; MMS-118P) at a dilution of 1:6000 and secondary anti-mouse IgG (whole molecule) peroxidase antibody (MilliporeSigma, St. Louis, MO, USA; A9044) at a dilution of 1:20 000 were used for the detection of YFP fusion proteins. Anti-His and anti-HA-Tag monoclonal primary antibodies and secondary antibody (HRP-conjugate) (ThermoFisher, Thermo Fisher Scientific, Waltham, MA, USA; Catalog# MA1-135; 26183; 31430) were used according to the manufacturers' recommendations for western blotting.

A. thaliana infection with *Botrytis cinerea*

Botrytis cinerea strain cultivation and plant infection was performed as described (Lionetti *et al.*, 2017).

Activity-based protein profiling

Proteins from root samples were extracted by grinding the roots in an 1.5 mL tube and were quantitatively analyzed by photometric measurement using the RC DC™ Protein Assay (Pharmacia LKB Ultraspec III Spectrophotometer) at 750 nm to ensure equal amounts of proteins in each sample during subsequent steps.

The probes used for ABPP were provided by the van der Hoorn lab at the Department of Plant Sciences of Oxford University. Labelling was performed by incubating the extracted proteins in 50 µL containing 125 mM 2-amino-2-(hydroxymethyl)-1,3-propanediol (TRIS) buffer (pH 7.5), 25 mM dithiothreitol (DTT) and 2 µM MV151 for 3–4 h at room temperature in the dark. In the case of competition labeling, the samples were pre-incubated with E64 (50 µM) for 30 min prior to labeling with the probe. The same volume of dimethyl sulphoxide (DMSO) was used as a non-probe control. After incubation, the labeled

proteins were separated on 12% SDS gels and visualized by in-gel fluorescence scanning using a Typhoon FLA 9000 scanner. Fluorescence intensity was measured using the ImageQuant TL software (GE Healthcare Life Sciences, <http://www.gelifescience.com>).

ACKNOWLEDGEMENTS

We thank Marena Henkle (Bartz) for technical assistance. This work was supported by Hatch Act and State of Iowa funds and by grants to T.J.B. from the Iowa Soybean Association, the North Central Soybean Research Program, and the United States Department of Agriculture NIFA-AFRI (Grant No. 2015-67013-23511).

CONFLICT OF INTERESTS

The authors declare there is no conflict of interest.

ACCESSION NUMBERS

Sequence data from this article can be found in the *A. thaliana* Genome Initiative or GenBank/EMBL databases under the following accession numbers: Hs4E02 (AF473826), MEKK1 (AT4G08500), PAD4 (AT3G52430), EDS1 (AT3G48090), WRKY40 (AT1G80840), PR1 (AT2G14610), PDF1.2 (AT5G44420), RD21A (AT1G47128).

AUTHOR CONTRIBUTIONS

GVP, PSJ, WBR, and TJB conceived and designed the experiments. GVP, PSJ, WBR, MH, FMWG, VL, and OAZ performed the experiments. GVP, PSJ, TRM, TH, JP, RALH, SS, VL, and TJB analyzed the data. RALH, SS, and OAZ contributed new reagents/analytic tools. GVP, PSJ, and TJB wrote the article with input from all authors.

SUPPORTING INFORMATION

Additional Supporting Information may be found in the online version of this article.

Figure S1. qRT-PCR expression analysis of the transgene in three independently transformed non-segregating *A. thaliana* lines constitutively expressing *Hs4E02*.

Figure S2. Alignment of RD21A yeast two-hybrid clones with the full-length protein.

Figure S3. Yeast (AH109 strain) co-transformation with selected RD21A interactors.

Table S1. List of gene-specific primers used in this work.

REFERENCES

- An, G., Ebert, P.R., Mitra, A. and Ha, S.B. (1988) Binary vectors. In *Plant Molecular Biology Manual*. Dordrecht, Belgium A3: Kluwer Academic Publishers, pp. 1–19.
- Bar-Ziv, A., Levy, Y., Citovsky, V. and Gafni, Y. (2012) The tomato yellow leaf curl virus (TYLCV) V2 protein interacts with the host papain-like cysteine protease CYP1. *Plant Signal Behav.* 7(8), 983–989.
- Baum, T.J., Wubben, M.J.E., Hardy, K.A., Su, H. and Rodermeil, S.R. (2000) A screen for *Arabidopsis thaliana* mutants with altered susceptibility to *Heterodera schachtii*. *J. Nematol.* 32, 166–173.
- Bernoux, M., Timmers, T., Jauneau, A., Brière, C., de Wit, P.J., Marco, Y. and Deslandes, L. (2008) RD19, an Arabidopsis cysteine protease required for RRS1-R-mediated resistance, is relocalized to the nucleus by the *Ralstonia solanacearum* PopP2 effector. *Plant Cell.* 20(8), 2252–2264.
- Biere, A. and Govere, A. (2016) Plant-mediated systemic interactions between pathogens, parasitic nematodes, and herbivores above- and belowground. *Annu. Rev. Phytopathol.* 54, 499–527.

- Bozkurt, T.O., Schornack, S., Win, J. et al. (2011) *Phytophthora infestans* effector AVRblb2 prevents secretion of a plant immune protease at the haustorial interface. *Proc. Natl Acad. Sci. USA*, **108**(51), 20832–20837.
- Burton, R.A., Gidley, M.J. and Fincher, G.B. (2010) Heterogeneity in the chemistry, structure and function of plant cell walls. *Nat. Chem. Biol.* **6**, 724–732.
- Chakravarthy, S., Velasquez, A.C. and Martin, G.B. (2009) Assay for pathogen-associated molecular pattern (PAMP)-triggered immunity (PTI) in plants. *J. Vis. Exp.* **31**, 1442.
- Chung, S.M., Frankman, E.L. and Tzfira, T. (2005) A versatile vector system for multiple gene expression in plants. *Trends Plant Sci.* **10**(8), 357–361.
- Clough, S.J. and Bent, A.F. (1998) Floral dip: a simplified method for Agrobacterium-mediated transformation of *Arabidopsis thaliana*. *Plant J.* **16**(6), 735–743.
- Cobb, N.A. (1914) *Nematodes and their relationships*. Yearbook of the Department of Agriculture. Washington DC: Department of Agriculture. pp. 457–490.
- Cravatt, B.F., Wright, A.T. and Kozarich, J.W. (2008) Activity-based protein profiling: from enzyme chemistry. *Annu. Rev. Biochem.* **77**, 383–414.
- Davies, L., Lei Zhang, L. and Elling, A. (2015) The *Arabidopsis thaliana* papain-like cysteine protease RD21 interacts with a root-knot nematode effector protein. *Nematology*, **17**, 655–666.
- Dixon, M.S., Golstein, C., Thomas, C.M., van Der Biezen, E.A. and Jones, J.D. (2000) Genetic complexity of pathogen perception by plants: the example of Rcr3, a tomato gene required specifically by Cf-2. *Proc. Natl Acad. Sci. USA*, **97**(16), 8807–8814.
- Edgington, L.E., Berger, A.B., Blum, G., Albrow, V.E., Paulick, M.G., Lineberry, N. and Bogyo, M. (2009) Non-invasive optical imaging of apoptosis using caspase-targeted activity based probes. *Nat. Med.* **15**, 967–973.
- Elling, A.A., Davis, E.L., Hussey, R.S. and Baum, T.J. (2007) Active uptake of cyst nematode parasitism proteins into the plant cell nucleus. *Int. J. Parasitol.* **37**(11), 1269–1279.
- Fabro, G., Steinbrenner, J., Coates, M. et al. (2011) Multiple candidate effectors from the oomycete pathogen *Hyaloperonospora arabidopsidis* suppress host plant immunity. *PLoS Pathog.* **7**(11), e1002348.
- Gao, B., Allen, R., Maier, T., Davis, E.L., Baum, T.J. and Hussey, R.S. (2001) Identification of putative parasitism genes expressed in the esophageal gland cells of the soybean cyst nematode *Heterodera glycines*. *Mol. Plant–Microbe Interact.* **14**(10), 1247–1254.
- Gao, B., Allen, R., Maier, T., Davis, E.L., Baum, T.J. and Hussey, R.S. (2003) The parasitome of the phytonematode *Heterodera glycines*. *Mol. Plant Microbe. Int.* **16**(8), 720–726.
- Ghosh, I., Hamilton, A.D. and Regan, L. (2000) Antiparallel leucine zipper-directed protein reassembly: application to the green fluorescent protein. *J. Am. Chem. Soc.* **122**(23), 5658–5659.
- Gu, C., Kolodziejek, I., Misas-Villamil, J., Shindo, T., Colby, T., Verdoes, M., Richau, K.H., Schmidt, J., Overkleef, H.S. and van der Hoorn, R.A. (2010) Proteasome activity profiling: a simple, robust and versatile method revealing subunit-selective inhibitors and cytoplasmic, defense-induced proteasome activities. *Plant J.* **62**, 160–170.
- Gu, C., Shabab, M., Strasser, R., Wolters, P.J., Shindo, T., Niemer, M., Kaschani, F., Mach, L. and van der Hoorn, R.A.L. (2012) Post-translational regulation and trafficking of the granulin-containing protease RD21 of *Arabidopsis thaliana*. *PLoS ONE*, **7**, 1–10.
- Habash, S.S., Radakovic, Z.S., Vankova, R., Siddique, S., Dobrev, P., Gleason, C., Grundler, F.M.W. and Elashry, A. (2017a) *Heterodera schachtii* tyrosinase-like protein – a novel nematode effector modulating plant hormone homeostasis. *Sci. Rep.* **7**(1), 6874.
- Habash, S.S., Sobczak, M., Siddique, S., Voigt, B., Elashry, A. and Grundler, F.M.W. (2017b) Identification and characterization of a putative protein disulfide isomerase (HsPDI) as an alleged effector of *Heterodera schachtii*. *Sci. Rep.* **7**(1), 13536.
- Hanada, K., Tamai, M., Yamagishi, M., Ohmura, S., Sawada, J. and Tanaka, I. (1978) Isolation and characterization of E-64, a new thiol protease inhibitor. *Agric. Biol. Chem.* **42**, 523–528.
- Hatsugai, N., Iwasaki, S., Tamura, K., Kondo, M., Fuji, K., Ogasawara, K., Nishimura, M. and Hara-Nishimura, I. (2009) A novel membrane-fusion-mediated plant immunity against bacterial pathogens. *Gene Dev.* **23**, 2496–2506.
- Hayashi, Y., Yamada, K., Shimada, T., Matsushima, R., Nishizawa, N.K., Nishimura, M. and Hara-Nishimura, I. (2001) A proteinase-storing body that prepares for cell death or stresses in the epidermal cells of *Arabidopsis*. *Plant Cell Physiol.* **42**(9), 894–899.
- Hezewi, T. (2015) Cellular signaling pathways and posttranslational modifications mediated by nematode effector proteins. *Plant Physiol.* **169**(2), 1018–1026.
- Hezewi, T. and Baum, T.J. (2013) Manipulation of plant cells by cyst and root-knot nematode effectors. *Mol. Plant–Microbe Interact.* **26**(1), 9–16.
- Hezewi, T., Howe, P., Maier, T.R., Hussey, R.S., Mitchum, M.G., Davis, E.L. and Baum, T.J. (2008) Cellulose binding protein from the parasitic nematode *Heterodera schachtii* interacts with *Arabidopsis* pectin methyltransferase: cooperative cell wall modification during parasitism. *Plant Cell.* **20**(11), 3080–3093.
- Holtmann, B., Kleine, M. and Grundler, F.M.W. (2000) Ultrastructure and anatomy of nematode-induced syncytia in roots of susceptible and resistant sugar beet. *Protoplasma*, **211**(1–2), 39–50.
- Hussey, R.S. (1989) Monoclonal antibodies to secretory granules in esophageal glands of *Meloidogyne* species. *J. Nematol.* **21**(3), 392–398.
- Jefferson, R.A., Kavanagh, T.A. and Bevan, M.W. (1987) GUS fusions: betaglucuronidase as a sensitive and versatile gene fusion marker in higher plants. *EMBO J.* **6**, 3901–3907.
- Jones, J.D. and Dangl, J.L. (2006) The plant immune system. *Nature*, **444**, 323–329.
- Juvalle, P.S. and Baum, T.J. (2018) ‘Cyst-ained’ research into *Heterodera* parasitism. *PLoS Pathog.* **14**(2), e1006791.
- Kandath, P.K., Ithal, N., Recknor, J., Maier, T., Nettleton, D., Baum, T.J. and Mitchum, M.G. (2011) The Soybean Rhg1 locus for resistance to the soybean cyst nematode *Heterodera glycines* regulates the expression of a large number of stress- and defense-related genes in degenerating feeding cells. *Plant Physiol.* **155**(4), 1960–1975.
- Kaschani, F., Verhelst, S.H.L., van Swieten, P.F., Verdoes, M., Wong, C.S., Wang, Z., Kaiser, M., Overkleef, H.S., Bogyo, M. and van der Hoorn, R.A. (2009) Minitags for small molecules: detecting targets of reactive small molecules in living plant tissues using ‘click chemistry’. *Plant J.* **57**, 373–385.
- Kaschani, F., Shabab, M., Bozkurt, T., Shindo, T., Schornack, S., Gu, C., Ilyas, M., Win, J., Kamoun, S. and van der Hoorn, R.A. (2010) An effector-targeted protease contributes to defense against *Phytophthora infestans* and is under diversifying selection in natural hosts. *Plant Physiol.* **154**(4), 1794–1804.
- Koenning, S.R. and Wrather, J.A. (2010) Suppression of soybean yield potential in the continental United States by plant diseases from 2006 to 2009. *Plant Health Prog.* <https://doi.org/10.1094/PHP-2010-1122-01-RS>.
- LampI, N., Alkan, N., Davydov, O. and Fluhr, R. (2013) Set-point control of RD21 protease activity by AtSerpin1 controls cell death in *Arabidopsis*. *Plant J.* **74**(3), 498–510.
- Lionetti, V., Fabri, E., De Caroli, M., Hansen, A.R., Willats, W.G., Piro, G. and Bellincampi, D. (2017) Three pectin methyltransferase inhibitors protect cell wall integrity for *Arabidopsis* immunity to *Botrytis*. *Plant Physiol.* **173**(3), 1844–1863.
- Liu, X., Liu, S., Jamai, A., Bendahmane, A., Lightfoot, D.A., Mitchum, M.G. and Meksem, K. (2011) Soybean cyst nematode resistance in soybean is independent of the Rhg4 locus LRR-RLK gene. *Funct. Integr. Gen.* **11**(4), 539–549.
- Livak, K.J. and Schmittgen, T.D. (2001) Analysis of relative gene expression data using real-time quantitative PCR and the 2(-Delta Delta C(T)) Method. *Methods.* **25**(4), 402–408.
- Lozano-Torres, J.L., Wilbers, R.H.P., Gawronski, P. et al. (2012) Dual disease resistance mediated by the immune receptor Cf-2 in tomato requires a common virulence target of a fungus and a nematode. *Proc. Natl Acad. Sci. USA*, **109**, 10119–10124.
- Lozano-Torres, J.L., Finkers-Tomczak, A., Schaik, C.C., Warmerdam, S., Schots, A., Bakker, J., Goverse, A. and Smant, G. (2014) Papain-like Cysteine proteases affect nematode susceptibility of tomato and *Arabidopsis* through plant cell wall-associated and jasmonic acid-dependent defence responses. Dissertation/PhD Thesis no. 5756. Wageningen University, Record number 2058226, ISBN 9789461739193, (5):129–149.
- Misas-Villamil, J.C., van der Hoorn, R.A. and Doehlemann, G. (2016) Papain-like cysteine proteases as hubs in plant immunity. *New Phytol.* **212**(4), 902–907.
- Mitchum, M.G. (2016) Soybean resistance to the soybean cyst nematode *Heterodera glycines*: an update. *Phytopathology*, **106**(12), 1444–1450.

- Mitchum, M.G., Hussey, R.S., Baum, T.J., Wang, X., Elling, A.A., Wubben, M. and Davis, E.L. (2013) Nematode effector proteins: an emerging paradigm of parasitism. *New Phytol.* **199**(4), 879–894.
- Mueller, A.N., Ziemann, S., Treitschke, S., Assmann, D. and Doehlemann, G. (2013) Compatibility in the *Ustilago maydis*-maize interaction requires inhibition of host cysteine proteases by the fungal effector Pit2. *PLoS Pathog.* **9**(2), e1003177.
- Noon, J.B., Hewezi, T., Maier, T.R. *et al.* (2015) Eighteen new candidate effectors of the phytonematode *Heterodera glycines* produced specifically in the secretory esophageal gland cells during parasitism. *Phytopathology*, **105**(10), 1362–1372.
- Noon, J.B., Qi, M., Sill, D.N., Muppirala, U., Eves-van den Akker, S., Maier, T.R., Dobbs, D., Mitchum, M.G., Hewezi, T. and Baum, T.J. (2016) A *Plasmodium*-like virulence effector of the soybean cyst nematode suppresses plant innate immunity. *New Phytol.* **212**(2), 444–460.
- Patel, N., Hamamouch, N., Li, C., Hussey, R., Mitchum, M., Baum, T., Wang, X. and Davis, E. (2008) Similarity and functional analyses of expressed parasitism genes in *Heterodera schachtii* and *Heterodera glycines*. *J. Nematol.* **40**(4), 299–310.
- Penninckx, I.A., Eggermont, K., Schenk, P.M., Van den Ackerveken, G., Cammue, B.P. and Thomma, B.P. (2003) The Arabidopsis mutant *top1* exhibits induced over-expression of the plant defensin gene PDF1.2 and enhanced pathogen resistance. *Mol. Plant Pathol.* **4**(6), 479–486.
- Pogorelko, G., Fursova, O., Lin, M., Pyle, E., Jass, J. and Zabolina, O.A. (2011) Post-synthetic modification of plant cell walls by expression of microbial hydrolases in the apoplast. *Plant Mol. Biol.* **77**(4–5), 433–445.
- Pogorelko, G., Lionetti, V., Fursova, O., Sundaram, R.M., Qi, M., Whitham, S.A., Bogdanove, A.J., Bellincampi, D. and Zabolina, O.A. (2013) *Arabidopsis* and *Brachypodium distachyon* transgenic plants expressing *Aspergillus nidulans* acetyltransferases have decreased degree of polysaccharide acetylation and increased resistance to pathogens. *Plant Physiol.* **162**(1), 9–23.
- Pogorelko, G.V., Mokryakova, M., Fursova, O.V., Abdeeva, I., Piruzian, E.S. and Bruskin, S.A. (2014) Characterization of three *Arabidopsis thaliana* immunophilin genes involved in the plant defense response against *Pseudomonas syringae*. *Gene*, **538**(1), 12–22.
- Pogorelko, G., Juvalle, P.S., Rutter, W.B., Hewezi, T., Hussey, R., Davis, E.L., Mitchum, M.G. and Baum, T.J. (2016a) A cyst nematode effector binds to diverse plant proteins, increases nematode susceptibility and affects root morphology. *Mol. Plant Pathol.* **17**(6), 832–844.
- Pogorelko, G.V., Kambakam, S., Nolan, T., Foudree, A., Zabolina, O.A. and Rodermeil, S.R. (2016b) Impaired chloroplast biogenesis in *immutans*, an *Arabidopsis* variegation mutant, modifies developmental programming, cell wall composition and resistance to *Pseudomonas syringae*. *PLoS ONE*, **11**(4), e0150983.
- Reem, N.T., Pogorelko, G., Lionetti, V., Chambers, L., Held, M.A., Bellincampi, D. and Zabolina, O.A. (2016) Decreased polysaccharide feruloylation compromises plant cell wall integrity and increases susceptibility to necrotrophic fungal pathogens. *Front. Plant Sci.* **7**, 630.
- Richau, K.H., Kaschani, F., Verdoes, M., Pansuriya, T.C., Niessen, S., Stuber, K., Colby, T., Overkleeft, H.S., Bogyo, M. and Van der Hoorn, R.A. (2012) Subclassification and biochemical analysis of plant papain-like cysteine proteases displays subfamily-specific characteristics. *Plant Physiol.* **158**(4), 1583–1599.
- Scheller, H.V. and Ulvskov, P. (2010) Hemicelluloses. *Annu. Rev. Plant Biol.* **61**, 263–289.
- Shindo, T., Misas-Villamil, J.C., Hörger, A.C., Song, J. and van der Hoorn, R.A. (2012) A role in immunity for Arabidopsis cysteine protease RD21, the ortholog of the tomato immune protease C14. *PLoS ONE*, **7**(1), e29317.
- Siddique, S., Sobczak, M., Tenhaken, R., Grundler, F.M. and Bohlmann, H. (2012) Cell wall ingrowths in nematode induced syncytia require UGD2 and UGD3. *PLoS ONE*, **7**(7), e41515.
- Siddique, S., Matera, C., Radakovic, Z.S., Hasan, M.S., Gutbrod, P., Rozanska, E., Sobczak, M., Torres, M.A. and Grundler, F.M. (2014) Parasitic worms stimulate host NADPH oxidases to produce reactive oxygen species that limit plant cell death and promote infection. *Sci. Signal.* **7**(320), ra33.
- Smakowska-Luzan, E., Mott, G.A., Parys, K. *et al.* (2018) An extracellular network of Arabidopsis leucine-rich repeat receptor kinases. *Nature*, **553**(7688), 342–346.
- Tamura, K., Shimada, T., Ono, E., Tanaka, Y., Nagatani, A., Higashi, S.I., Watanabe, M., Nishimura, M. and Hara-Nishimura, I. (2003) Why green fluorescent fusion proteins have not been observed in the vacuoles of higher plants. *Plant J.* **35**(4), 545–555.
- Vanholme, B., Mitreva, M., Van Criekinge, W., Logghe, M., Bird, D., McCarter, J.P. and Gheysen, G. (2006) Detection of putative secreted proteins in the plant-parasitic nematode *Heterodera schachtii*. *Parasitol. Res.* **98**, 414–424.
- Verdoes, M., Florea, B.I., Menendez-Benito, V. *et al.* (2006) A fluorescent broad-spectrum proteasome inhibitor for labeling proteasomes *in vitro* and *in vivo*. *Chem. Biol.* **13**, 1217–1226.
- Wieczorek, K., Golecki, B., Gerdes, L. *et al.* (2006) Expansins are involved in the formation of nematode-induced syncytia in roots of *Arabidopsis thaliana*. *Plant J.* **48**(1), 98–112.
- Xu, X.M., Lin, H., Maple, J., Bjorkblom, B., Alves, G., Larsen, J.P. and Moller, S.G. (2010) The Arabidopsis DJ-1a protein confers stress protection through cytosolic SOD activation. *J. Cell Sci.* **123**(Pt 10), 1644–1651.
- Yamada, K., Matsushima, R., Nishimura, M. and Hara-Nishimura, I. (2001) A slow maturation of a cysteine protease with a granulin domain in the vacuoles of senescing Arabidopsis leaves. *Plant Physiol.* **127**(4), 1626–1634.
- Zabolina, O., Malm, E., Drakakaki, G., Bulone, V. and Raikhel, N. (2008) Identification and preliminary characterization of a new chemical affecting glucosyltransferase activities involved in plant cell wall biosynthesis. *Mol. Plant.* **1**, 977–989.